PHYSICAL REVIEW B VOLUME 51, NUMBER 19 15 MAY 1995-I

Ab initio calculations of SiC(110) and GaAs(110) surfaces: A comparative study and the role of ionicity

Magdalena Sabisch, Peter Krüger, and Johannes Pollmann
Institut für Theoretische Physik II, Universität Münster, D-48149 Münster, Germany
(Received 11 October 1994; revised manuscript received 30 December 1994)

We report *ab initio* calculations of structural and electronic properties of β-SiC and of the nonpolar SiC(110) surface. The calculations are carried out self-consistently in the local-density approximation employing smooth norm-conserving pseudopotentials in separable form. Gaussian orbital basis sets are used for an efficient description of the wave functions. These are strongly localized at the carbon atoms, in particular. For the bulk crystal 40 Gaussians per unit cell with s, p, d, and s^* symmetry are found to be sufficient for good convergence. Our results for the SiC ground-state structural parameters and the bulk band structure are in excellent agreement with the results of previous plane-wave calculations and with experimental data. We scrutinize the character of the chemical bond in SiC by comparisons with diamond, Si, GaAs, and ZnS, which have been investigated on equal footing. The SiC(110) surface is described in a supercell geometry. The optimal surface relaxation is determined by eliminating the forces iteratively. We find a top-layer bond-length-*contracting* rotation relaxation in which the Si surface layer atoms move closer towards the substrate while the C surface-layer atoms relax only parallel to the ideal surface plane. SiC(110) exhibits an occupied and an empty dangling-bond band within the fundamental gap. The occupied band predominantly originates from the dangling bonds at the surface carbon atoms which behave like anions. The empty band mainly originates from the dangling bonds at the surface Si atoms which act as cations. We present and discuss our results for the SiC(110) surface in direct comparison with the GaAs(110) surface. Further comparisons with literature data on surfaces of more ionic II-VI compounds like ZnS or ZnO are given, as well. This allows us to address the physical origins of the surface relaxation behavior of these compound semiconductors and to identify characteristic differences and similarities in the relaxation which are related to the specific types of heteropolarity or ionicity of these systems.

I. INTRODUCTION

In recent years structural and electronic properties of cubic and hexagonal polytypes of bulk SiC have been studied by first-principles investigations.[1-5] Conversely, the surface properties of various SiC polytypes so far have been studied mostly by semiempirical methods, [for SiC(110) see, e.g., Refs. 6-8]. Only very recently has the geometric structure of SiC(110) been calculated self-consistently by Wenzien, Käckell, and Bechstedt,[9] and preliminary results on its surface electronic structure were reported by these authors.[10] The main driving force for the renaissance in interest in SiC polytypes and their surfaces is their paramount potential for microelectronic devices,[11-13] in particular for high-temperature, high-power and high-frequency applications.[11] The strong bonding between Si and C atoms in SiC makes this material very resistant to high-temperature and radiation damage. In view of this extraordinary application potential a thorough knowledge of the structural and electronic properties of SiC and its surfaces is a matter of both basic interest and technological importance.

First-principles calculations of the electronic and structural properties of SiC using modern *ab initio* pseudopotentials require an enormous number of plane-wave basis states for a convergent description because of the strong C $2p$ potential which gives rise to strongly localized $2p$ orbitals at the C atoms. A proper description of the C $2p$ electrons therefore enforces a very extensive numerical effort when a plane-wave basis is employed. For cubic bulk SiC, Chang and Cohen[1] observed that a basis of 1200 plane waves is needed for good convergence, and Wenzien, Käckell, and Bechstedt[9,10] used an energy cutoff of 30 Ry, corresponding to 8200 plane waves, for the SiC(110)-(1×1) surface. We have studied cubic SiC and the SiC(110) surface using smooth pseudopotentials and localized Gaussian basis sets. For the bulk calculations 40 Gaussian orbitals per unit cell turn out to be sufficient for good convergence,[14] and an extension of our approach to supercell calculations for surfaces is then straightforward. We have to employ 400×400 matrices only to describe convergently the structural and electronic properties of the SiC(110) surface. The nonpolar SiC(110) surface is an ideal prototype system for an *ab initio* study of the relaxation behavior and electronic properties of a SiC surface. Surface charging effects, as encountered, e.g., for polar SiC(100) surfaces, are avoided this way.

SiC shows a number of similarities with heteropolar covalent compound semiconductors like GaAs. But it shows distinct differences from heteropolar covalent semiconductors, as well. We have studied bulk GaAs and the GaAs(110) surface for comparison. In addition, it is very revealing to compare SiC and its (110) surface with some heteropolar ionic materials like ZnS or ZnO. We have reported self-consistent studies of heteropolar

 ©1995 The American Physical Society

ionic II-VI compounds[15] and their nonpolar surfaces[16] previously. A direct comparison of all of these results allows us to scrutinize the influence of the specific type and origin of ionicity in SiC on its bulk and surface properties. On the Phillips scale,[17] SiC has a much lower ionicity ($f_i=0.177$) than, e.g., GaAs ($f_i=0.310$) or ZnS ($f_i=0.623$). However, the appropriateness of this scale for compound semiconductors containing second-row elements has been discussed critically recently by Garcia and Cohen.[18] These authors suggested using the asymmetry of the charge density along the bonds of binary compounds as a measure of ionicity. Their ionicity is consequently based on the first-principles charge density along the anion-cation bond. The respective g values, as defined in Ref. 18 for GaAs ($g=0.316$), SiC ($g=0.475$), and ZnS ($g=0.673$) are close to the Phillips ionicity for GaAs and ZnS but indicate a considerably larger ionicity of SiC as compared to the Phillips scale. The ionicity of bulk SiC has also been addressed by Chang and Cohen,[1] by Karch *et al.*,[5] and by Lambrecht and Segall.[19] On the basis of our first-principles results we complement that discussion for bulk SiC and extend it in considerable depth to the structural and electronic properties of a prototypical SiC surface.

In this paper we present results of our *ab initio* pseudopotential calculations of ground-state properties of bulk cubic SiC and its nonpolar (110) surface. These include the bulk lattice constant, the bulk modulus, the bulk electronic structure, the optimal surface relaxation, the surface electronic structure, and the electron affinity. To investigate the ionicity of SiC, we discuss the total bulk valence-charge distribution of C, Si, GaAs, SiC, and ZnS and representative charge distributions of salient surface states for the SiC(110) and GaAs(110) surfaces in comparison.

The paper is organized as follows: In Sec. II we briefly summarize the framework of our calculations, and present the smooth pseudopotentials employed in our studies. In Sec. III we apply these pseudopotentials and Gaussian basis sets to a convergent description of bulk cubic SiC. We find that a basis set as small as 40 Gaussian orbitals per unit cell yields results that are virtually identical with available state-of-the-art plane-wave results. In this section we address, in addition, similarities and differences in the total valence-charge density of SiC as compared to C, Si, GaAs, and ZnS. Section IV is devoted to the presentation and a detailed discussion of the surface structural and electronic properties of SiC(110) in comparison with our respective results for GaAs(110), and for nonpolar surfaces of II-VI semiconductors. The physical origin of the relaxation behavior of the different surfaces is addressed. A short summary concludes the paper in Sec. V.

II. METHOD OF CALCULATION

In this section, we briefly summarize the calculation scheme of our studies and we address, in particular, the pseudopotentials which we employ.

A. Calculational framework

Our calculations are carried out in the framework of density-functional theory within the local-density approximation[20] (LDA). We have employed the Ceperley-Alder[21] form of the exchange and correlation potential (XC potential) as parametrized by Perdew and Zunger.[22] Nonlocal, norm-conserving pseudopotentials in separable form, as suggested by Kleinman and Bylander,[23] are used. They will be addressed in more detail in Sec. II B. The wave functions are expanded in terms of linear combinations of Gaussian orbitals of s, p, d and s^* symmetry types. In the calculations of the bulk charge density we use ten special **k** points in the irreducible part of the bulk Brillouin zone (BBZ) according to the special-point scheme of Chadi and Cohen.[24] For the (110) surface we employ four special $\mathbf{k}_{\parallel}$ points in the irreducible part of the surface Brillouin zone (SBZ). The total energy is calculated self-consistently using the momentum-space formalism of Ihm, Zunger, and Cohen.[25] The optimal surface relaxation is determined within the supercell approach. For both GaAs(110) and β-SiC(110) we employ nine atomic layers and five vacuum layers in the supercell. We optimize the structure by calculating the forces. When a Gaussian basis is employed, Pulay forces have to be taken into account in addition to the Hellmann-Feynman forces.[26] Eliminating the forces iteratively is achieved by employing the Broyden scheme.[27] We move all atoms in the unit cell until all forces vanish within 10^{-3} Ry/a.u.

B. Pseudopotentials

Our calculations for GaAs have been carried out using the Ga^{3+} and As^{5+} ionic pseudopotentials of Stumpf, Gonze, and Scheffler,[28] in the separable Kleinman-Bylander form. These pseudopotentials are very smooth, and the respective bulk pseudo-wave-functions can be represented by 20 Gaussian orbitals per atom of s, p, d and s^* symmetries with decay constants as given in Table I. Our ground-state structural parameters of GaAs as resulting with 40 Gaussian orbitals per unit cell are in excellent agreement with the plane-wave results of Alves, Hebenstreit, and Scheffler[29] and with experimental data.[30] The theoretical (experimental) lattice constant and bulk modulus are 5.54 Å (5.65 Å) and 0.869 Mbar (0.769 Mbar), respectively.

For SiC we employ norm-conserving pseudopotentials which we have constructed in a separate study[14] accord-

TABLE I. Decay constants of the Gaussian orbitals for C, Si, Ga, and As as used in the present calculations.

	Decay constants for surface-layer atoms ($1/\text{a.u.}^2$)	Decay constants for bulk and substrate layer atoms ($1/\text{a.u.}^2$)
C	0.25, 1.0, 2.86	0.35, 1.7
Si	0.18, 0.5, 1.0	0.20, 0.6
Ga	0.16, 0.5, 1.0	0.19, 0.5
As	0.16, 0.5, 1.0	0.19, 0.5

ing to the nonrelativistic prescription as given by Hamann, Schlüter, and Chiang.[31] Since there are no p electrons in the carbon core, the p part of the nonlocal C^{4+} pseudopotential usually comes out to be very strong. This is, e.g., the case for the C^{4+} potential of Stumpf, Gonze, and Scheffler[28] (SGS potential) which is shown in Fig. 1(a). Obviously such a p potential calls for a large basis set to represent the respective wave functions convergently. Our much smoother (in particular, the p component) C^{4+} pseudopotential is shown in Fig. 1(b). It was constructed by using three different core radii. The nonlocal s and p parts of our potential have been determined from the ground-state configuration $1s^2 2s^2 2p^2$ of carbon with core radii $r_{cs}=0.75$ a.u. and $r_{cp}=0.74$ a.u. For the d part, we have used the ion configuration $1s^2 2s^{0.75} 2p^1 3d^{0.25}$ with core radius $r_{cd}=0.82$ a.u., since the d states are not bound in the ground state. After constructing the potential this way it was transformed into a separable form according to Kleinman and Bylander.[23] The resulting relatively smooth pseudopotential yields very accurate ground-state structural parameters and band-structure energies for bulk diamond. Using a 40 Gaussian orbital basis set (for the decay constants, see Table I) we obtain 3.52 Å (3.57 Å) for the lattice constant and 4.33 Mbar (4.42 Mbar) for the bulk modulus, in very good agreement with the experimental data[30] given in parentheses. The band structures of bulk diamond calculated with 40 or 80 Gaussian orbitals per unit cell in the basis are virtually identical, and are in very close agreement with the results of a 749 plane-wave calculation.[32]

The pseudopotential of Si, a third-row element, is less critical. The SGS potential[28] is already very smooth. Our potential, constructed according to Hamann, Schlüter, and Chiang,[31] turns out to be very similar.[14] Both the SGS pseudopotential and our pseudopotential consequently yield very similar results for the structural and electronic properties of bulk Si. In our calculations a basis set of 40 Gaussian orbitals per unit cell with decay constants as given in Table I turns out to be sufficient for good convergence. We obtain 5.38 Å (5.43 Å) for the lattice constant and 1.183 Mbar (0.988 Mbar) for the bulk modulus. The experimental data[30] are given in parentheses for comparison. Our calculated band-structure energies agree very closely with the results of a 400-plane-wave calculation by Fiorentini.[33]

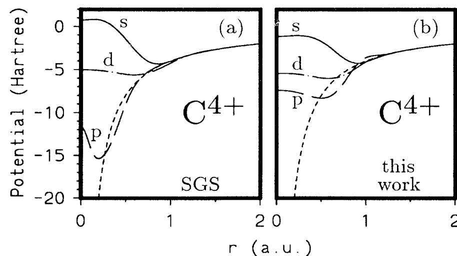

FIG. 1. Nonlocal ionic pseudopotential for C^{4+} from Stumpf, Gonze, and Scheffler (SGS, Ref. 28) in comparison with our smooth ionic pseudopotential. The dashed line shows the potential $-4/r$ (in atomic units) in each case.

Having checked the appropriateness of our 40 Gaussian orbital basis sets and of our C^{4+} pseudopotential for bulk diamond and our Si^{4+} pseudopotential for bulk Si, we can now combine the two to study SiC.

III. BULK CUBIC SiC

In this section we present our results for cubic SiC in comparison with the results of previous self-consistent calculations and experimental data. Furthermore we contrast the properties of β-SiC with those of GaAs and other elemental and compound semiconductors in order to highlight similarities and differences of these semiconductors. This will define the starting point for our *ab initio* calculations of the nonpolar (110) surfaces of GaAs and SiC to be reported in Sec. IV.

A. Structural properties

Using our C^{4+} and Si^{4+} pseudopotentials for bulk SiC we obtain convergent results with 40 Gaussian orbitals per unit cell. The calculated lattice constants and bulk moduli for SiC as resulting from our calculations for different sizes of the Gaussian basis sets and different exchange-correlation potentials are compared in Table II with respective theoretical and experimental literature data. To allow for a more complete comparison, we have carried out bulk SiC calculations as well, using the Wigner XC potential.[34] The table convincingly reveals

TABLE II. Lattice constants and bulk moduli for cubic SiC resulting from our calculations with 40 and 70 GO basis sets. For comparison the results of plane wave (PW) calculations and full potential-linear combination of muffin-tin orbitals (FP-LMTO) calculations, as well as experimental data, are given. The calculations have been carried out for the Wigner, Ceperley-Alder or von Barth–Hedin XC potentials.

SiC	Lattice constant (Å)	Bulk modulus (Mbar)
Wigner		
40 GO	4.38	2.16
70 GO	4.37	2.10
PW[a]	4.36	2.12
PW[b]	4.36	2.19
Ceperley-Alder		
40 GO	4.34	2.26
70 GO	4.33	2.22
PW[c]	4.34	2.22
PW[b]	4.35	2.20
von Barth-Hedin		
FP-LMTO[d]	4.32	2.23
experiment	4.36[e]	2.24[f]

[a]Reference 1.
[b]Reference 4.
[c]Reference 5.
[d]Reference 3.
[e]References 30 and 36.
[f]References 35 and 36.

that our results obtained with only 40 Gaussian orbitals per unit cell are in excellent agreement with converged plane-wave results both for the Wigner and Ceperley-Alder forms of the XC potential, respectively. The differences between our results for 70 and 40 Gaussians per unit cell are so small that the smaller basis set can be used for the SiC surface calculations without significant loss of accuracy. We note in passing that Table II highlights the type of agreement that is reached nowadays in fully converged self-consistent calculations of ground-state structural properties of SiC.

B. Band structure

In Table III we compare our band-structure energies at high-symmetry points, as obtained with 40 Gaussian orbitals per unit cell, with other theoretical results from the literature. Experimental data are given for further reference. The comparison clearly shows that the 40 Gaussian basis set used together with our smooth pseudopotentials yields results which agree excellently with plane-wave and linear-muffin-tin-orbital atomic-sphere-approximation (LMTO-ASA) results from the literature. They agree with experimental data as accurately as one can expect for LDA results. Conduction-band states are much better described by *GW* quasiparticle calculations, as is well known from the work of Hybertsen and Louie.[39] Our recent *GW* calculations have yielded quasiparticle energies for SiC which are in excellent agreement with experimental data (see Ref. 40 for that matter).

The band structures of SiC and GaAs resulting from our calculations are shown in direct comparison in Fig. 2. We observe three salient differences. First, the width of the SiC valence bands amounts to 15.2 eV, while it is only 12.9 eV for GaAs. This is due to the extraordinary strength of the C 2*p* potential. Second, the heteropolar gap in GaAs is direct and its width is 3.4 eV, while it is indirect in SiC with a width of 1.5 eV only. Third, and most importantly, GaAs is a direct-gap semiconductor while SiC is indirect with a gap between the Γ_{15v} valence band and the X_{1c} conduction band. Comparing the two band structures in the energy region of the conduction bands, it becomes immediately obvious that the conduction bands are also largely similar in nature and dispersion except for the lowest conduction band, in particular along the Δ-symmetry line from Γ to X. Here the relatively larger strength of the carbon potential with respect to Si, as compared to the As potential with respect to Ga, draws the cationic *s*-like conduction band to lower energies between Γ and X. It should be noted at this point that both band structures in Fig. 2 have been calculated for the theoretical lattice constant. The gap in GaAs is known to be extremely sensitive with respect to the lattice constant used in the calculations.[41] This is not the case for SiC. It is thus merely fortuitous that our calculated gap for GaAs almost agrees with the measured gap. In SiC the deviation between $E_g^{\mathrm{th}}=1.29$ eV and $E_g^{\mathrm{expt}}=2.417$ eV shows the usual LDA underestimation of the gap energy. All above-mentioned properties, of course, have a direct influence on the respective surface structural and electronic properties of GaAs(110) and SiC(110), as will be discussed in Sec. III C.

From Secs. III A and III B we conclude that our pseudopotentials for Si and C together with a basis set as small as 40 Gaussians per unit cell yield structural and

TABLE III. Band-structure energies (in eV) of cubic SiC, calculated for the theoretical lattice constant, using our smooth pseudopotentials together with a 40 GO basis set. Plane-wave and LMTO-ASA results from the literature are given for comparison. The last column shows experimental data for further reference. An energy separation of 7.5 eV between L_{3v} and L_{1c} has been determined in Ref. 38. We have included the difference between this value and the measured L_{3v} value as the experimental L_{1c} energy of 6.34 eV in the table.

SiC	This work	PW[a]	LMTO-ASA[b]	Expt.
Γ_{1v}	−15.51	−15.36	−15.45	
Γ_{15v}	0.00	0.00	0.00	0.00
Γ_{1c}	6.38	6.27	6.31	7.4[c]
Γ_{15c}	7.13	7.07	7.76	
X_{1v}	−10.39		−10.33	
X_{3v}	−7.86		−7.88	
X_{5v}	−3.24		−3.24	−3.4[c]
X_{1c}	1.29	1.21	1.39	2.417[c]
X_{3c}	4.30		4.66	4.7[d], 5.5[d]
X_{5c}	13.85			
L_{1v}	−11.86		−11.81	
L_{1v}	−8.64		−8.71	
L_{3v}	−1.09		−1.01	−1.16[d]
L_{1c}	5.44	5.32	5.58	4.2[d], 6.34[c]
L_{3c}	7.17		8.09	8.5[d]
L_{1c}	10.19			
E_{gap}	1.29	1.21	1.39	2.417[c]

[a]Reference 1.
[b]Reference 37.
[c]Reference 38.
[d]Reference 36.

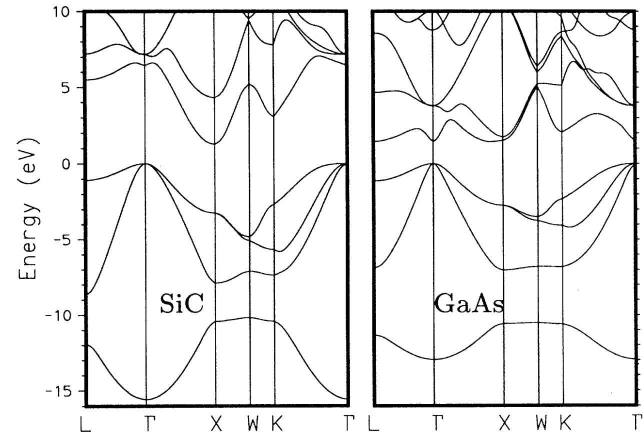

FIG. 2. Electronic bulk band structure of cubic SiC and GaAs, calculated at the theoretical lattice constants, in direct comparison.

electronic properties of bulk SiC which are as good as state-of-the-art results from the literature.

C. Ionicity

We now digress for a brief discussion of the heteropolarity or ionicity of SiC. In particular, we want to identify similarities and differences with respect to these quantities between SiC and usual heteropolar semiconductors like GaAs or ZnS. We have already mentioned that the ionicities of SiC, GaAs, and ZnS on the Phillips scale are 0.177, 0.310, and 0.623, respectively. We will present more detailed evidence in this subsection for placing SiC between GaAs and ZnS with respect to ionicity, further supporting the meaningfulness of using the asymmetry of the charge density of binary compounds and the respective g values as a complementary measure of ionicity as suggested by Garcia and Cohen.[18] SiC, GaAs, and ZnS are all ionic to a certain extent, but the origin of the respective ionicities is largely different in SiC from that of GaAs and ZnS. The latter compounds are heterovalent with three (two) valence electrons per cation and five (six) valence electrons per anion, respectively, while SiC is homovalent with four valence electrons per cation and anion. In contrast to GaAs or ZnS, the ionicity of SiC is believed to originate from the difference in core size (or covalent radius) of C and Si. This core-size difference results in an asymmetric electronic charge distribution about the midpoint of the Si—C bond. In Fig. 3 we compare charge density contours of SiC with those of the two homopolar covalent semiconductors diamond and Si, which are the constituents of SiC, as well as with those of GaAs and ZnS. These charge densities have all been calculated on equal footing within our approach and can, therefore, be directly compared quantitatively. For ZnS the Zn^{2+} and S^{6+} pseudopotentials given in Ref. 15 have been employed. The contours in Fig. 3 are shown in increments of 2.5 electrons per unit cell volume and the lowest density contour corresponds to the same value. To ease the quantitative comparison, we show in Fig. 4 the respective charge densities along the [111] direction containing the anion-cation bond. The figures show how the charge density is distributed between the two atoms forming the chemical bond for each semiconductor. Diamond and Si show symmetric distributions, as is typical for homopolar covalent semiconductors. Si exhibits a pronounced bond charge about the midpoint of the bond, while the bond charge of diamond is characterized by a double peak (see top panel of Fig. 4 for that matter), as was discussed, e.g., by van Camp, Van Doren, and Devreese[42] already. Considering Figs. 3 and 4, we clearly see that the charge density increases around the anion site at the expense of the charge density around the cation site when we move from GaAs to ZnS. The charge-density maximum or bond charge is shifted concomitantly away from the midpoint of the bond toward the anion. Figure 3 clearly reveals that SiC lies between GaAs and ZnS with respect to its charge-density asymmetry. This notion is further confirmed by Fig. 4, which shows that the charge-density maximum in the respective bonds increases from GaAs over SiC to ZnS. There is, however, one salient quantitative difference to be noted in Fig. 4 between SiC and the other two compound semiconductors which is of considerable importance for the relaxation behavior of the respective (110) surfaces to be discussed below. The bond-charge maximum between anion and cation in GaAs and ZnS is at 32% and 27% of the respective bond lengths away from the anion. In SiC, on the contrary, it is only 20% of the bond length away from the anion, showing that the charge density of SiC stronger resembles that of a more ionic crystal (see, e.g., the respective result[15] for ZnO, where the bond-charge maximum is only 13% of the bond length away from the anion). This similarity is related to the fact that both SiC and ZnO contain anions from the second row of the Periodic Table whose core radii or covalent radii are much smaller than those of the respective cations. This is

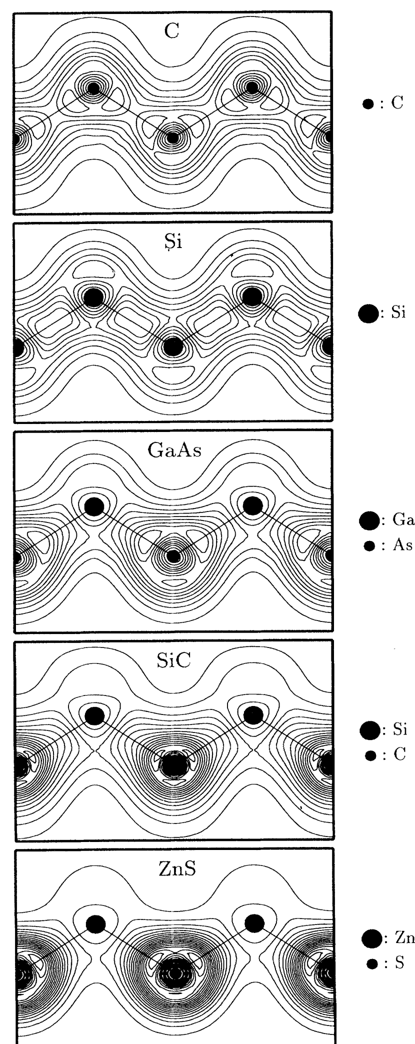

FIG. 3. Total valence-charge-density contours in a [001]-[110] plane for C, Si, GaAs, SiC, and ZnS. The increments of the contours are $2.5e$ per unit cell. The lowest contour has this value in each case. The respective bond lengths are used as length units in each panel.

not the case for GaAs or ZnS, for which the anions and cations have similar covalent radii. The stronger shift of the bond charge toward the anion in SiC as compared to GaAs or ZnS becomes even more transparent when we decompose the charge densities of the compound semiconductors in Fig. 4 along the anion-cation bonds into their symmetric and antisymmetric components according to Garcia and Cohen.[18] The result is shown in Fig. 5.

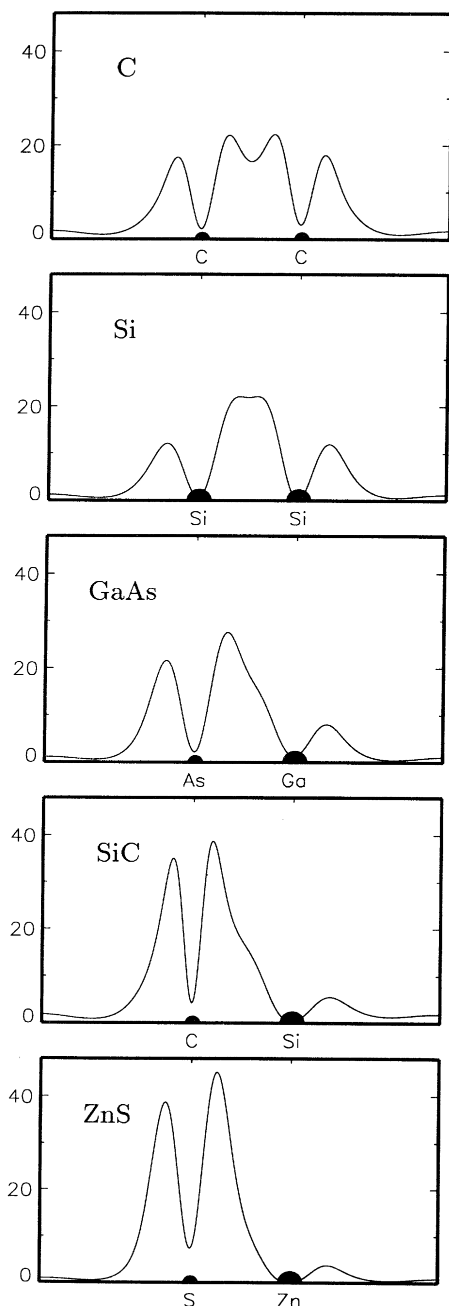

FIG. 4. Total valence-charge densities along the [111] direction of C, Si, GaAs, SiC, and ZnS in e per unit cell. The positions of anions and cations along this direction are indicated, and the respective bond lengths are used as length units in each case.

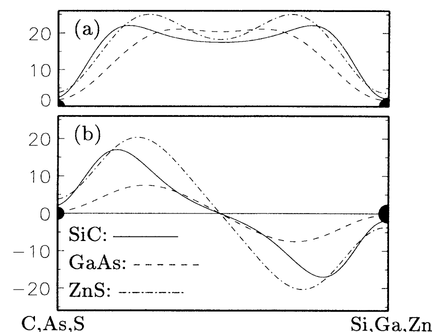

FIG. 5. Symmetric and antisymmetric components of the total valence charge densities of GaAs, SiC, and ZnS along the anion-cation bonds (in e per unit cell). The bond lengths are used as length units in each case.

First we observe that all three compounds have a strong antisymmetric component in their charge density. Second we see that the maximums position in the antisymmetric components of GaAs and ZnS occur at similar relative distances from the anion. Third, the absolute value of the maximum of the antisymmetric component for ZnS is almost three times as large as that of GaAs, explaining the much larger ionicity of the former semiconductor. Finally, the absolute value of the maximum of the antisymmetric component of SiC is more than twice as large as that of GaAs but smaller than that of ZnS, placing SiC between these two compounds with respect to ionicity. Most importantly the maximum position is shifted closer to the anion in SiC than in GaAs or ZnS, explaining why SiC behaves more like a heteropolar ionic than a heteropolar covalent semiconductor. All these observations are of direct relevance for the quantitative differences in the relaxation behavior of the nonpolar surfaces of these compound semiconductors to be discussed below.

In conclusion of this subsection, our results corroborate in detail the placement of SiC between GaAs and ZnS with respect to their ionicities, as was suggested by the respective g values of Garcia and Cohen.[18] The experimental gap energies of GaAs ($E_g = 1.52$ eV), cubic SiC ($E_g = 2.417$ eV), and cubic ZnS ($E_g = 3.8$ eV) further confirm this notion. Our calculations yield g values of 0.302, 0.475, and 0.676 for GaAs, SiC, and ZnS, respectively, which are very close to those given in Ref. 18. An alternative ionicity scale based on LMTO calculations by Lambrecht and Segall[19] also finds SiC to be more ionic than GaAs and less ionic than typical II-IV semiconductors such as ZnSe.

IV. THE SiC(110) SURFACE IN COMPARISON WITH GaAs(110)

In this section we present our first-principles results for the nonpolar β-SiC(110) surface, and discuss its structural and electronic properties in comparison with those of GaAs(110) and of other II-VI compound semiconductors. First we briefly summarize our results for GaAs(110).

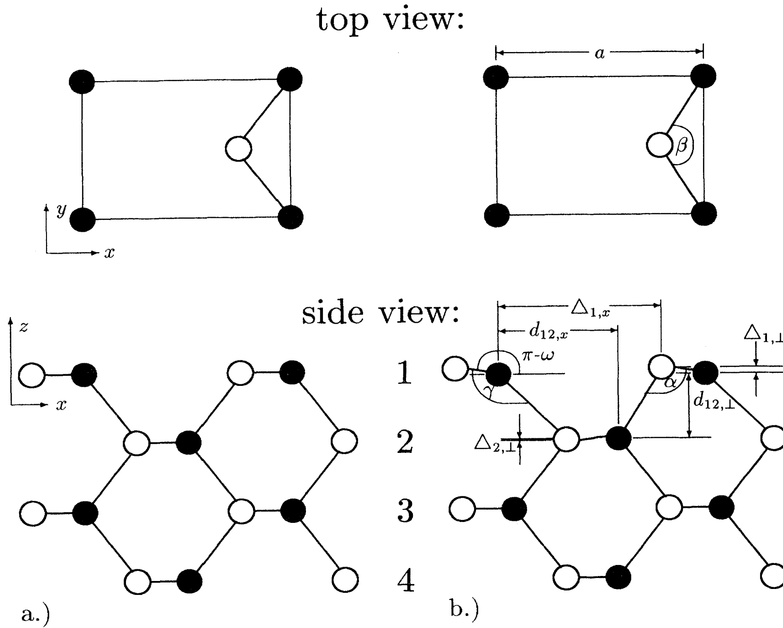

FIG. 6. Top and side views of an ideal and a relaxed (110) surface of a zinc-blende semiconductor (schematic). The structure parameters shown in (b) are used to characterize the relaxation (see text). Anions and cations are shown by open circles and full dots, respectively. The side views show the first four layers (1–4) at the surface. The axes x, y, and z refer to the crystallographic directions [001], [$\bar{1}$10], and [110], respectively.

A. The GaAs(110) surface: a brief summary

The GaAs(110) surface is one of the well-known and most intensively studied surfaces.[43] We summarize our results for this surface only very briefly in comparison with those of the most recent *ab initio* pseudopotential calculation by Alves, Hebenstreit, and Scheffler[29] in order to establish the appropriateness of our approach for surfaces as well.

The structure of the ideal and relaxed GaAs(110) surfaces is shown schematically by top and side views in Fig. 6. The structure parameters commonly used (see, e.g., Refs. 44 and 45) to characterize the relaxation are defined in Fig. 6(b). In our structure optimizations we have relaxed the upper and lower four layers of the nine atomic layers in each unit cell. The middle layer was fixed in its bulk configuration with the theoretical lattice constant of 5.54 Å. We have used the SGS pseudopotentials[28] for Ga^{3+} and As^{5+} and the Ceperley-Alder[21] form of the XC potential. The wave functions on the top layers of each slab were expanded in terms of 30 Gaussians per atom, while the wave functions localized on all other atoms in the slab were described by 20 Gaussians per atom (for the decay constants see Table I). This leads to 400×400 slab Hamiltonian matrices.

In Table IV we compare our structure parameters with those calculated by Alves, Hebenstreit, and Scheffler[29] and those measured by Duke *et al.*[44] and Tong, Wei, and Xu.[45] Alves, Hebenstreit, and Scheffler used a supercell geometry with eight atomic and six vacuum layers employing the SGS pseudopotentials and the Ceperley-Alder XC potential as well, and a plane-wave basis set. Thus differences in our results and those of Alves, Hebenstreit and Scheffler essentially only result from the different basis sets employed. Our results in Table IV show very good agreement with the theoretical results of Ref. 29, as well as with measured data[44,45] confirming the appropriateness of our relatively small Gaussian basis sets. We find the well-known top-layer bond-length-conserving rotation relaxation model[43] in which the As surface-layer atoms relax outward while the Ga surface-layer atoms relax inward. The relaxation of the second-layer atoms is already very small.

Our surface electronic structure of the ideal and the relaxed GaAs(110)-(1×1) surfaces, which we show in Fig. 7 for a later comparison with SiC(110), shows the well-known behavior upon surface relaxation. The occupied anion-derived As dangling-bond band A_5 moves to lower energy and the empty cation-derived Ga dangling-bond band C_3 moves to higher energy, clearing the gap from surface states. The energy gain per unit cell due to relax-

TABLE IV. Calculated structure parameters for the relaxed GaAs(110) surface as resulting from our work in comparison with the plane-wave results of Alves, Hebenstreit, and Scheffler and with experimental data. For the definition of the structure parameters, see Fig. 6.

GaAs(110)	This work	Alves, Hebenstreit, and Scheffler[a]	Duke *et al.*[b]	Tong, Wei, and Xu[c]
a_b (Å)	5.54	5.56	5.65	5.65
d_b (Å)	2.40	2.41	2.45	2.45
$\Delta_{1,\perp}(d_b)$	0.29	0.28	0.28	0.28
$\Delta_{1,x}(d_b)$	1.82	1.83	1.84	1.78
$\Delta_{12,\perp}(d_b)$	0.60	0.59	0.59	0.60
$d_{12,x}(d_b)$	1.34	1.32	1.36	1.29
$\Delta_{2,\perp}(d_b)$	−0.04	−0.04	−0.02	−0.01
ω (deg)	30.6	30.2	31.1	28.0

[a]Reference 29.
[b]Reference 44.
[c]Reference 45.

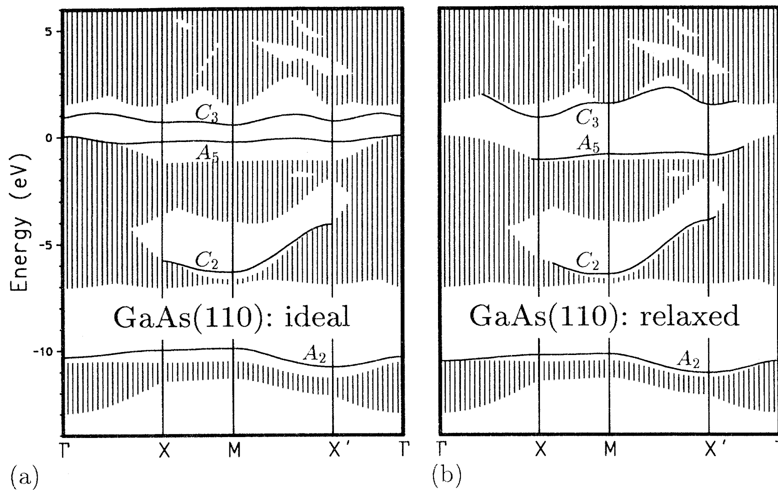

FIG. 7. Salient bands of localized surface states of ideal (a) and relaxed (b) GaAs(110) surfaces together with the projected bulk band structure.

ation amounts to $\Delta E = 0.80$ eV.

The charge densities of the anion-derived dangling-bond state (A_5) and the cation-derived dangling-bond state (C_3) at the M point of the SBZ are shown in the left and right panels of Fig. 8, respectively. The figures clearly reveal the localized nature and the origin of the related states.

Our calculated energy values of localized surface states are in excellent agreement (all within 0.1 eV) with the results of Alves, Hebenstreit, and Scheffler, and agree with experimental data as good as those (see Ref. 29 for that matter).

From these comparisons we conclude that our calculational procedure yields structural and electronic properties for the GaAs(110) surface which are in very good agreement with well-converged results[29,46] from the literature.

B. The β-SiC(110) surface

In this subsection we first address the structure of the relaxed β-SiC(110) surface and the physical origins of the surface relaxation. Then we present the electronic structure of the ideal and relaxed surfaces as resulting from our self-consistent calculations. To our knowledge, no low-energy electron-diffraction (LEED) studies have been published for this surface to date.

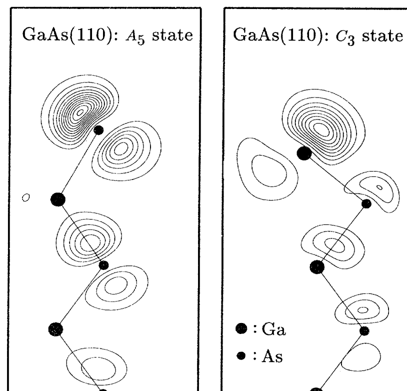

FIG. 8. Charge densities of the As- and Ga-derived dangling-bond states A_5 and C_3 at the M point of the relaxed GaAs(110) surface.

1. Surface structure

The ideal β-SiC(110) surface has the same atomic configuration as the GaAs(110) surface [see Fig. 6(a)]. Surface-layer atoms are threefold coordinated, while all bulk atoms are fourfold coordinated. We have carried out our structure optimization calculations for SiC(110) in the same way as for GaAs(110), using the theoretical bulk lattice constant $a_b = 4.34$ Å. The C^{4+} and Si^{4+} pseudopotentials discussed in Sec. II B were employed together with the Ceperley-Alder form of the XC potential. Also in this case we employed 30 Gaussians per surface layer atom and 20 Gaussians per atom in the slab (for the decay constants see Table I). Thus we again have to deal with 400×400-slab Hamiltonian matrices.

The relaxation geometry calculated self-consistently in this work is given in Table V together with the results of a recent self-consistent structure optimization by Wenzien, Käckell, and Bechstedt[9,10] and semiempirical calculations by Lee and Joannopoulos[6] as well as by Mehandru and Anderson.[8] Our calculated structure shows a top-layer bond-length-contracting rotation relaxation in which the C surface atoms only relax parallel to the surface while the Si surface atoms relax parallel and perpendicular to the surface. The latter move down by 0.25 Å toward the substrate. The relaxation of the atoms on the following layers is very small. For the convenience of the reader, we give the absolute displacements of the Si and C atoms on the first two layers relative to their positions at the ideal surface. The displacements Δx in the x direction are -0.202 Å for Si(1), $+0.039$ Å for C(1), 0.011 Å for Si(2), and 0.033 Å for C(2). The respective displacements Δz in the z direction are -0.252 Å for Si(1), 0.004 Å for C(1), 0.052 Å for Si(2), and 0.015 Å for C(2). On the third and fourth layers, the displacements are less or equal to 0.01 Å.

TABLE V. Calculated structure parameters for the relaxed SiC(110) surface (see Table IV and Fig. 6 for reference). Our results are compared to those of one previous self-consistent (Ref. 10) and two previous empirical-tight-binding (Refs. 6 and 8) structure optimizations.

SiC(110)	This work	Wenzien, Käckell, and Bechstedt[a]	Lee and Joannopoulos[b]	Mehandru and Anderson[c]
a_b (Å)	4.34	4.29	4.36	4.36
d_b (Å)	1.88	1.86	1.89	1.89
$\Delta_{1,\perp}(d_b)$	0.14	0.13	0.06	0.05
$\Delta_{1,x}(d_b)$	1.86	1.82	1.82	1.86
$d_{12,\perp}(d_b)$	0.65	0.67	0.73	0.71
$d_{12,x}(d_b)$	1.27	1.27	1.24	1.21
$\Delta_{2,\perp}(d_b)$	−0.02	−0.02	−0.01	−0.01
ω (deg)	16.9	15.4	7.4	6.0

[a]Reference 10.
[b]Reference 6.
[c]Reference 8.

Our results are in very close agreement with the structural parameters as obtained by Wenzien, Käckell, and Bechstedt[9,10] in their plane-wave calculations. Comparing our results with those of the semiempirical tight-binding calculations, there are significant quantitative differences to be noted (see Table V). Still the qualitative relaxation behavior as calculated by Lee and Joannopoulos[6] and Mehandru and Anderson[8] is largely similar to that in our results. Those authors also find the Si atoms to move closer to the substrate than the C atoms. In their results, however, the C atoms do not stay within the ideal surface layer but slightly relax toward the substrate by 0.05 and 0.12 Å, respectively. The calculations by Takai, Halicioglu, and Tiller[7] yield a qualitatively different relaxation. According to their calculations, the C atoms move closer to the substrate than the Si atoms. This is at variance with other theoretical results, and with the general physical and chemical picture of the relaxed surface to be developed below. The energy gain due to relaxation turns out to be $\Delta E = 0.64$ eV per unit cell in our results, a value that compares extremely well with the respective value of $\Delta E = 0.63$ eV as obtained by Wenzien, Käckell, and Bechstedt.[9,10] Mehandru and Anderson[8] obtained, as well, a value of $\Delta E = 0.64$ eV, while Lee and Joannopoulos[6] found a smaller value of $\Delta E = 0.42$ eV. As mentioned already, these structural results are predictions, since there are no experimental data available in the literature, to our knowledge.

2. Physical origin of the surface relaxation

We now want to discuss our energy-optimized surface structure of SiC(110) in comparison with those of the nonpolar GaAs(110), ZnS(110), and ZnO(10$\bar{1}$0) surfaces in order to identify similarities and differences in the relaxation behavior of these surfaces. In particular, we want to scrutinize the physical origin of the relaxation behavior of these systems. GaAs and ZnS are heteropolar covalent while SiC and ZnO are heteropolar ionic, as discussed in Sec. III C. The latter compounds are both distinguished by having anions from the second row of the Periodic Table. In Fig. 9 we show side views of the optimal relaxation geometries of GaAs(110), SiC(110), and ZnO(10$\bar{1}$0) as resulting from this work and from our previous calculation.[16] ZnS(110) shows a very similar relaxation behavior to GaAs(110) (see, e.g., Ref. 43). In Table VI we present bond lengths (see Fig. 9 for their definition) and bond angles that characterize these geometries. First we note that the relaxation angle ω at the SiC(110) surface turns out to be 16.9° only, as com-

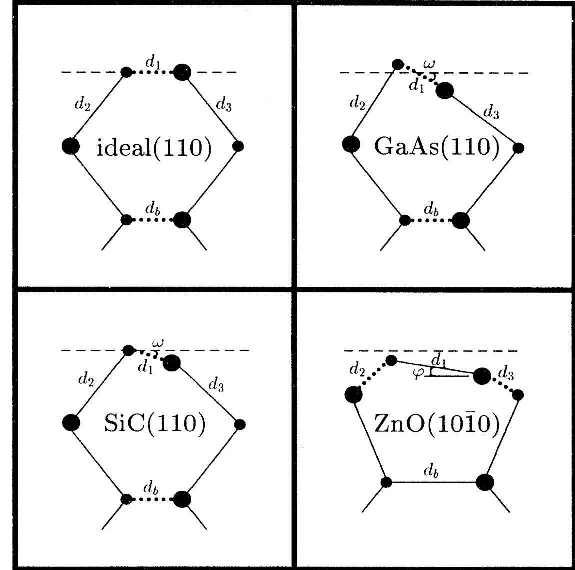

FIG. 9. Side views (drawn to scale) of an ideal zinc-blende (110) surface and of the energy-optimized relaxed GaAs(110), SiC(110), and ZnO(10$\bar{1}$0) surfaces. The ideal surface plane is indicated by a dashed line in each case. Bonds that form an angle with the drawing plane are shown by dotted lines. Bonds which lie in the drawing plane or which are parallel to the drawing plane are shown by full lines. Small dots show anions, while large dots show cations. The actual values of the bond lengths d_1, d_2, and d_3 at the surface, the bulk bond lengths d_b, as well as the relaxation angles ω and the tilt angles φ are given in Table VI.

TABLE VI. Bulk and surface bond lengths, relaxation and tilt angles (see Fig. 9), and bond angles (see Sec. IV B 2) of an ideal zinc-blende (110) surface and of the relaxed GaAs(110), SiC(110), and ZnO($10\bar{1}0$) surfaces (for details, see text).

	Ideal	GaAs(110)	SiC(110)	ZnO($10\bar{1}0$)[a]
d_b (Å)	$a_b\sqrt{3}/4$	2.40	1.88	1.99
$d_1(d_b)$	1.00	0.99	0.94	0.92
$d_2(d_b)$	1.00	1.01	0.99	0.96
$d_3(d_b)$	1.00	0.99	0.97	0.94
ω (deg)	0	30.6	16.9	3.6
φ (deg)	0	16.7	8.2	3.6
α (deg)	109.5	89.0	99.8	
β (deg)	109.5	110.8	120.2	
γ (deg)	109.5	124.1	116.4	

[a]Reference 16.

pared to the value of 30.6° for GaAs and 28° for ZnS (see Ref. 43). For ZnO($10\bar{1}0$) we have calculated[16] a tilt angle of the Zn—O surface-layer bond with respect to the surface plane of 3.6°. It should be noted at this point that the relaxation angle ω, commonly used to characterize (110) zinc-blende surfaces, is the angle between the surface plane and the projection of the anion-cation bond onto the [110]-[$1\bar{1}0$] plane which is used for the side-view plots of the structure (see, e.g., Fig. 6). The tilt angle φ, on the contrary, is the actual angle between the surface-layer bond and the surface plane. Since at ZnO($10\bar{1}0$), the Zn—O surface layer bonds reside in the drawing plane (see Fig. 9) the relaxation angle ω and the tilt angle φ are identical. This is not the case for GaAs(110) and SiC(110), as is obvious from Fig. 9. The actual tilt angle φ at the GaAs(110) and SiC(110) surfaces is considerably smaller than the relaxation angle ω, and amounts to 16.7° and 8.2°, respectively. The resulting order of the calculated surface-layer-bond tilt angles φ in Table VI for GaAs(110), SiC(110), and ZnO($10\bar{1}0$) nicely corresponds to the increasing ionicities of these compounds, placing SiC between GaAs and ZnO again. In order to understand why these angles show the observed trend, we have to address the origins of the relaxation in more detail.

The specific relaxation behavior of a particular surface system, in general, is mostly the result of a combined action of different physical mechanisms. For the systems discussed in this paper we can identify at least three different competing mechanisms. They all influence the relaxation behavior of particular surfaces to a more or less strong extent. The first mechanism (I) which we observe in our results is that the less electronegative cations reside closer to the substrate than the more electronegative anions (see Fig. 9 for that matter). This is due to the fact that the kinetic energy of the valence electrons and their Coulomb repulsion energy is minimized when the more strongly charged surface-layer ion resides as high as possible above all other atoms. The more electronegative surface ions are thus positioned above the plane of the less electronegative surface ions. The second mechanism (II) is related to the different hybridization behavior of threefold-coordinated atoms at the surface as compared to the fourfold-coordinated bulk atoms. As suggested already by Lee and Joannopoulos,[6] it is energetically favorable for threefold-coordinated atoms with s^2p^1 or s^2p^2 valence-electronic configurations to attain a planar bonding configuration by sp^2 hybridization. However, since the second-layer atoms are constrained by the bulk lattice, the surface atoms are not able to assume an exactly planar geometry. The surface Ga atom, e.g., has a $4s^24p^1$ valence configuration, so that the energetically most favorable way of forming three chemical bonds is to promote one s electron to the p level and to form sp^2 hybrid bonds. Since the sp^2 hybrids form a planar configuration, the Ga surface-layer atoms are likely to be planar threefold coordinated. The As atoms, on the contrary, have a $4s^24p^3$ valence configuration, so that threefold-coordinated As tends to form pyramidal p^3 bonds. Si and C both have s^2p^2 valence configurations, so that threefold-coordinated Si and C are both likely to be planar bonded according to the valence argument given above. The third mechanism (III), finally, is related to the ionicity and, in particular, to the specific asymmetry of the charge densities in these compounds. As a matter of fact, it is not the absolute value of the maximum of the charge density along the anion-cation bond which is decisive for this mechanism but its localization on the connection line between the anion and cation. This becomes obvious by considering GaAs and ZnS as opposed to SiC and ZnO. GaAs and ZnS have different ionicities and different absolute values of the maximum in charge density along the anion-cation bond, but the maxima occur at similar relative positions along the bonds (see Figs. 4 and 5). In consequence both GaAs(110) and ZnS(110) show roughly the same relaxation behavior with roughly the same relaxation angle. For SiC(110) and ZnO($10\bar{1}0$) this angle is much smaller, as is shown in Table VI. This is related to the fact that the maximum position of the asymmetric charge density on the bonds essentially determines the stiffness and directionality of the bonding configuration at the surface. In the bulk, the tetrahedral configuration is defined by the total-energy minimum, resulting to a large extent from the interaction of a given ion with its four nearest neighbors. At the surface one neighbor of the anion (cation) is missing. The remaining three bonds only stay within a configuration corresponding to tetrahedral bonding if the Coulomb repulsion between the respective bond charges is large enough. If not, the topmost ion is free to move closer to its three neighbors, thereby contracting the three respective bonds. Considering only the electrostatic attraction between the ions, a planar configuration would yield the highest energy gain. The extent to which the bonds at the surface are contracted very critically depends on the localization of the bond charge on the anion-cation bond. The more the bond charge moves toward the anion, the more directional covalent bonding is relaxed in favor of nondirectional ionic bonding. For the Coulomb attraction between ions only their distance is of importance. To be more specific, the hybridization mechanism II is characterized by quantum-mechanical interactions, while the ionicity mechanism III is characterized by electrostatic interactions. The outcome of the combined effects of mechanisms II and III is thus the result of a tradeoff between quantum-mechanical and classical interactions.

In more covalent systems the quantum-mechanical interactions dominate, while in more ionic systems the classical interactions dominate.

We can now rationalize the specifically different relaxation behaviors of our considered systems by invoking the three mechanisms presented above. For GaAs and ZnS directional covalent bonding is still efficiently in action at the surface because the bond-charge maximum is still far away from the anions (32% and 27% of the relative distance for GaAs and ZnS, respectively) so that the surface-bond lengths remain almost bulklike (see Table VI). Mechanisms I and II both support an outward shift of the surface anions and an inward shift of the surface cations, as is observed in experiment and theory. Mechanism III is not yet very important. The similarity in the relaxation behaviors of GaAs(110) and ZnS(110), in spite of their different ionicities, can be rationalized this way. In SiC and ZnO, the bond-charge maximum has moved much closer to the anion as compared to GaAs or ZnS. Its distance from the anion is only 20% (13%) of the respective bond length in SiC (ZnO). The surface relaxation angles concomitantly become increasingly smaller, as pointed out already. The bond-contracting mechanism due to the strong shift of the bond charge toward the anion together with the first mechanism explains why both the anion and the cation at ZnO($10\bar{1}0$) move closer to the substrate, with the anions residing higher above the substrate than the cations. Since ionic nondirectional bonding becomes more dominant than covalent tetrahedral bonding, all bond lengths near the SiC(110) and ZnO($10\bar{1}0$) surface are contracted (see Table VI). Concerning the position of the anions, SiC(110) falls in between the clear-cut cases of GaAs(110) or ZnS(110) on the one hand and ZnO($10\bar{1}0$) on the other hand. Mechanism I supports the tendency of the C anions to move upward above the ideal surface plane, while mechanism II, in the case of the C anions at SiC(110), supports their downward relaxation closer to the substrate. In our results these competing mechanisms just happen to cancel leaving the C atoms within the surface plane. Wenzien, Käckell, and Bechstedt[10] found a slight outward displacement of the C atoms in their LDA calculations. The results of the semiempirical structure optimizations in Refs. 6 and 8 place the C anions slightly (0.05 and 0.12 Å, respectively) below the ideal surface plane. For the Si cations at SiC(110) all three mechanisms work in the same direction, allowing the cations to relax closer to the substrate in order to attain a planar threefold-coordinated sp^2 configuration as much as compatible with the total configuration. Our results for the bond lengths and bond angles in Table VI nicely confirm these expectations and thus corroborate the notion of the three mechanisms presented above to be in competing action at these surfaces. In the case of ZnO, finally, the bonds have become strongly ionic and the hybridization mechanism II loses its impact. Mechanisms I and III both support a contraction of the surface bonds and a movement of the Zn cations closer toward the substrate as compared to the O anions, as mentioned already. This behavior is clearly shown by the results of our calculations in Fig. 9 and Table VI.

Finally, we address the physical trends that can be observed in the bond angles at the surface. The angles defined by cations and anions on the first two layers are given as follows:

$$\alpha:\hat{=}c(2)-a(1)-c(1)$$

$$\beta:\hat{=}c(1)-a(1)-c(1) \text{ or } a(1)-c(1)-a(1)\ ,$$

$$\gamma:\hat{=}a(1)-c(1)-a(2)$$

We note at this point that these angles are qualitatively different at the (110) surface of a zinc-blende crystal and the ($10\bar{1}0$) surface of a Wurtzite crystal, so that a direct comparison of these angles resulting from the surface relaxation is not meaningful. However, we can follow the trends in these angles when we consider the relaxation of zinc-blende (110) surfaces alone. At ideal surfaces they all have the value 109.5° of the bulk tetrahedral angle. If the surface cations move closer to the substrate, the angle γ increases and the angle α decreases with respect to the ideal surface value. If the cation reaches an exactly planar configuration, γ would amount to 120° and α would amount to 90°, but the concomitant movement of the anions also changes these angles. If the bond lengths are conserved in the relaxation the angle β remains near 109.5°, but if the bond lengths are contracted the angle β opens up. Thus α is a measure for the upward shift of the anions and the downward shift of the cations, while β is a measure of bond contraction. The angle γ, finally, is a measure of sp^2 hybridization and the downward shift of the cation. Our results in Table VI clearly reveal the relaxation properties. At GaAs(110) the bonds are not contracted, so that β remains near the tetrahedral angle. At the same time α becomes much smaller (close to 90°) and γ becomes much larger (close to 120°) than the tetrahedral angle because of the sp^2 hybridization of the Ga cation and the upward motion of the As anion. For SiC(110), sp^2 hybridization is already considerably weaker and the C anions remain in the ideal surface plane. Thus both α and γ are much closer to the tetrahedral angle, as compared to GaAs(110), but the bond contraction at SiC(110) gives rise to a drastic increase in the value of β. For the even more ionic ZnO($10\bar{1}0$) surface the bond contraction at the surface is even further enhanced as is obvious from the bond lengths in Table VI. Finally we point out that an exact planar configuration of the cations at the surface gives rise to the largest possible tilt angle φ. Comparing the tilt angles for the three surfaces in Table VI clearly demonstrates that the cation at GaAs(110) reaches a position closest to planar bonding with the largest tilt angle φ and relaxation angle ω.

3. *Surface electronic structure*

Our surface electronic structure of the ideal and the relaxed SiC(110) surface is shown in Figs. 10(a) and 10(b), respectively. The topology of the projected bulk band structure is similar to that of GaAs(110) to a large extent. Only the projected heteropolar gap of SiC(110) is much smaller than that of GaAs(110). We find a number of salient bands of localized surface states both at the ideal

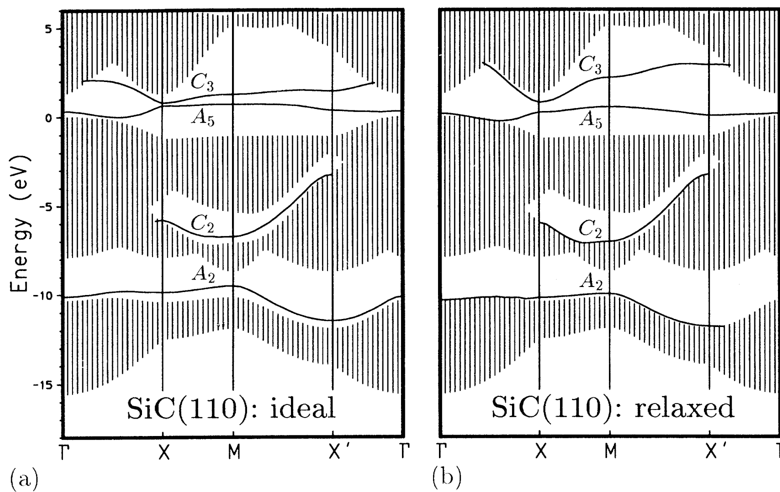

FIG. 10. Salient bands of localized surface states of ideal (a) and relaxed (b) SiC(110) surfaces together with the projected bulk band structure.

and relaxed surfaces. We have used the same labeling of these bands as in Fig. 7. The wave-function character of the related states at high-symmetry points of the relaxed surface is analyzed in Table VII. The A_2 state has a very appreciable cation contribution of 38% at M and even 51% at X', as compared to 36% at M and only 26% at X' for GaAs(110). This is a consequence of the much smaller heteropolar gap of SiC as compared to GaAs. Bands A_5 and C_3 predominantly originate from the dangling bonds at the C anion and Si cation in the surface layer. This is similar, in general, to GaAs(110). The energy separation of our A_5 and C_3 bands at the SiC(110) surface is considerably smaller as compared to GaAs(110). This is certainly related to the differences in calculated band gap energies as commented on in Sec. III B. Wenzien, Käckell, and Bechstedt[10] have reported dangling-bond surface-state bands in the gap, as well. These bands, which have been classified as preliminary in Ref. 10, show significant deviations from our results. The relaxed surface clearly is semiconducting, but our calculated indirect surface gap of about 0.3 eV is obviously much smaller than the calculated bulk gap of 1.29 eV. Thus the gap is not cleared from surface states by relaxation. Therefore, the relaxed SiC(110) surface will exhibit bona fide gap states and will not give rise to a flat-band situation as is the case for the GaAs(110) cleavage face or for the $(10\bar{1}0)$ surface[16] of the heteropolar ionic ZnO crystal. Our calculations yield an ionization energy of 5.42 eV and, correspondingly, an electron affinity of 4.13 eV. Comparing these values with our corresponding results of 4.65 and 3.21 eV, respectively, for GaAs(110), again indicates the larger ionicity of SiC as compared to GaAs.

To highlight the origin and nature of the most salient dangling-bond surface states at SiC(110), in Fig. 11 we show the charge densities of the A_5 and C_3 states at the M point. Clearly, the A_5 state is a dangling-bond state localized mostly at the C surface anions, and the C_3 state is a dangling-bond state localized mainly at the Si surface cations (see also Table VII). Also in this case, like for GaAs(110) in Fig. 8, we observe contributions from the anions (cations) on the third and fifth layers to the A_5 and C_3 states. Comparing Figs. 11 and 8 reveals one particular difference. While the A_5 state and the C_3 state at GaAs(110) are mainly localized at the As or Ga atoms on the first and third layers, at the SiC(110) surface the A_5

TABLE VII. Orbital contributions to salient surface states (in %) at high-symmetry points of the relaxed SiC(110) surface.

SiC(110)		C(2s)	C(2p)	C(3d)	Si(3s)	Si(3p)	Si(3d)
X	A_2	56.4	1.6	0.1	0.4	37.4	4.1
	A_5	6.7	69.6	1.3	0.8	5.9	15.7
	C_3	2.1	9.6	1.6	3.0	62.6	21.1
M	A_2	59.9	1.6	0.0	0.1	32.1	6.3
	C_2	0.3	40.0	2.7	54.8	0.7	1.5
	A_5	6.5	75.7	0.4	0.2	3.0	14.2
	C_3	2.3	16.3	4.4	7.9	57.6	11.5
X'	A_2	46.3	1.9	0.9	30.0	15.2	5.7
	A_5	7.9	69.5	0.8	1.0	5.9	14.9
	C_3	3.2	12.6	6.6	17.3	46.5	13.7

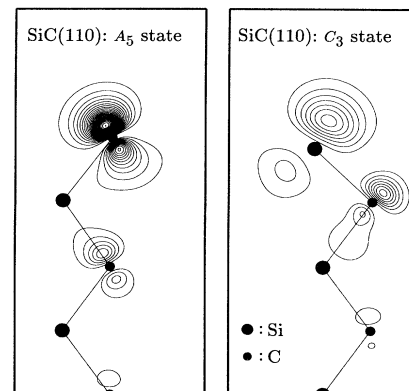

FIG. 11. Charge densities of the C- and Si-derived dangling-bond states A_5 and C_3 at the M point of the relaxed SiC(110) surface.

state is localized near the C atoms at the first and third layers while the C_3 state is localized on both the first-layer Si and second-layer C atoms. Thus the wave-function character of the C_3 state at SiC(110) is somewhat different from that of the C_3 state at GaAs(110). Concerning the similarities of Figs. 8 and 11, we clearly see that the C (Si) atoms at the SiC(110) surface behave like the As (Ga) atoms at the GaAs(110) surface.

V. SUMMARY

In conclusion, we have reported *ab initio* studies of bulk cubic SiC and of the SiC(110) surface, as well as of the GaAs(110) surface. Optimal surface geometries have been calculated by total-energy minimization. The GaAs(110) surface shows the well-known top-layer bond-length-conserving rotation relaxation, in which the As atoms relax outward and the Ga atoms relax inward with respect to the ideal surface plane and the substrate. The SiC(110) surface, on the contrary, shows a top-layer bond-length-contracting rotation relaxation similar to that of the ZnO($10\bar{1}0$) surface. The C surface atoms remain in the ideal surface plane, while the Si surface atoms relax inward toward the substrate by 0.25 Å. The length of the surface-layer Si—C bond is reduced to 1.77 Å, as opposed to the theoretical bulk bond length of 1.88 Å. A similar shortening of the surface-layer bond has previously been found for ZnO($10\bar{1}0$). It was shown to be typical for heteropolar ionic semiconductors like SiC and ZnO but does not occur for heteropolar covalent semiconductors like GaAs or ZnS. We have addressed different competing physical mechanisms whose combined action was found to give rise to the specific relaxation behavior observed. The topology of the surface band structures of SiC(110) and GaAs(110) are similar, although characteristic differences due to the different ionicity and due to the indirect fundamental gap of SiC do occur. Salient bands of localized surface states result throughout the whole SBZ. Most pronounced are the anion- and cation-derived dangling-bond bands which show significant energy shifts upon surface relaxation. The cation-derived dangling-bond state C_3 at SiC(110) shows a slightly different charge density as compared to the C_3 state at GaAs(110). For GaAs(110) our results are in very good agreement with available angle-resolved photoelectron spectroscopy and LEED data. For SiC(110) such data are still lacking. We hope that our predictions will motivate experimental studies of the SiC(110) surface in the near future.

ACKNOWLEDGMENTS

One of us (M.S.) would like to acknowledge support by the Bischöfliche Studienförderung, Cusanuswerk (Bonn, Germany). In addition, it is our pleasure to acknowledge fruitful discussions with A. Mazur and M. Rohlfing.

[1] K. J. Chang and M. L. Cohen, Phys. Rev. B **35**, 8196 (1987); B. H. Cheong, J. J. Chang, and M. L. Cohen, *ibid.* **44**, 1053 (1991).
[2] C. Cheng, R. J. Needs, and V. Heine, J. Phys. C **21**, 1049 (1988).
[3] W. R. L. Lambrecht, B. Segall, M. Methfessel, and M. van Schilfgaarde, Phys. Rev. B **44**, 3685 (1991).
[4] C. H. Park, B.-H. Cheong, K.-H. Lee, and K. J. Chang, Phys. Rev. B **49**, 4485 (1994).
[5] K. Karch, P. Pavone, W. Windl, D. Strauch, and F. Bechstedt, Int. J. Quantum Chem. (to be published).
[6] D. H. Lee and J. D. Joannopoulos, J. Vac. Sci. Technol. **21**, 351 (1982).
[7] T. Takai, T. Halicioglu, and W. A. Tiller, Surf. Sci. **164**, 341 (1985).
[8] S. P. Mehandru and A. B. Anderson, Phys. Rev. B **42**, 9040 (1990).
[9] B. Wenzien, P. Käckell, and F. Bechstedt, in *Proceedings of the 5th International Conference on Silicon Carbide and Related Materials, Washington, 1993,* edited by M. Spencer, IOP Conf. Proc. No. 137 (Institute of Physics and Physical Society, London, 1994), p. 223.
[10] B. Wenzien, P. Käckell, and F. Bechstedt, Surf. Sci. **307**, 989 (1994).
[11] R. F. Davis, Z. Sitar, B. E. Williams, H. S. Kong, H. J. Kim, J. W. Palmour, J. A. Edmond, J. Ryu, J. T. Glass, and C. H. Carter, Jr., Mater. Sci. Eng. B **1**, 77 (1988).
[12] W. J. Choyke, in *The Physics and Chemistry of Carbides, Nitrides and Borides,* Vol. 183 of *NATO Advanced Study Institute, Series E: Applied Sciences,* edited by R. Freer (Kluwer, Dordrecht, 1990), p. 563.
[13] G. Pensl and R. Helbig, in *Festkörperprobleme, Advances in Solid State Physics,* edited by U. Rössler (Vieweg, Braunschweig, 1990), Vol. 30, p. 133.
[14] M. Sabisch, Diploma thesis, Universität Münster, 1993.
[15] P. Schröer, P. Krüger, and J. Pollmann, Phys. Rev. B **47**, 6971 (1993); **48**, 18 264 (1993).
[16] P. Schröer, P. Krüger, and J. Pollmann, Phys. Rev. B **49**, 17 092 (1994).
[17] J. C. Phillips, *Bonds and Bands in Semiconductors* (Academic, New York, 1973).
[18] A. Garcia and M. L. Cohen, Phys. Rev. B **47**, 4215 (1993); **47**, 4221 (1993).
[19] W. R. L. Lambrecht and B. Segall, Phys. Rev. B **41**, 2832 (1990).
[20] P. Hohenberg and W. Kohn, Phys. Rev. **136**, B864 (1964); W. Kohn and L. J. Sham, *ibid.* **140**, A1133 (1965).
[21] D. Ceperley and B. J. Alder, Phys. Rev. Lett. **45**, 566 (1980).
[22] J. P. Perdew and A. Zunger, Phys. Rev. B **23**, 5048 (1981).
[23] L. Kleinman and D. M. Bylander, Phys. Rev. Lett. **48**, 1425 (1982).
[24] D. J. Chadi and M. L. Cohen, Phys. Rev. B **8**, 5747 (1973).
[25] J. Ihm, A. Zunger, and M. L. Cohen, J. Phys. C **12**, 4409 (1979).
[26] M. Scheffler, J. P. Vigneron, and G. Bachelet, Phys. Rev. B **31**, 6541 (1985); P. Krüger and J. Pollmann, Physica B **172**, 155 (1991).
[27] C. G. Broyden, Math. Comput. **19**, 577 (1965); see also D. D. Johnson, Phys. Rev. B **38**, 12 807 (1988).
[28] R. Stumpf, X. Gonze, and M. Scheffler (unpublished); X. Gonze, R. Stumpf, and M. Scheffler, Phys. Rev. B **44**, 8503 (1991).

[29]J. L. A. Alves, J. Hebenstreit, and M. Scheffler, Phys. Rev. B **44**, 6188 (1991).
[30]*Numerical Data and Functional Relationships in Science and Technology,* edited by K. H. Hellwege and O. Madelung, Landolt-Börnstein, New Series, Group III, Vol. 17, Pt. a and Vol. 22, Pt. a (Springer, Berlin, 1982).
[31]D. R. Hamann, M. Schlüter, and C. Chiang, Phys. Rev. Lett. **43**, 1494 (1979); Phys. Rev. B **32**, 393 (1984); D. Hamann, *ibid.* **40**, 2980 (1989).
[32]A. Mazur (private communication).
[33]V. Fiorentini, Phys. Rev. B **46**, 2086 (1992).
[34]E. Wigner, Trans. Faraday Soc. **34**, 678 (1938); Phys. Rev. **46**, 1002 (1937).
[35]D. H. Yean and J. R. Riter, Jr., J. Phys. Chem. Solids **32**, 653 (1971).
[36]W. von Münch, in *Numerical Data and Functional Relationships in Science and Technology,* edited by O. Madelung, M. Schulz, and H. Weiss, Landolt-Börnstein, New Series, Groups IV and III-V, Vol. 17, Pt. a (Springer, Berlin, 1982), and references therein.
[37]W. R. L. Lambrecht and B. Segall, Phys. Rev. B **43**, 7070 (1991).
[38]W. R. L. Lambrecht, B. Segall, M. Yoganathan, W. Suttrop, R. P. Devaty, W. J. Choyke, J. A. Edmond, J. A. Powell, and M. Alouani, Phys. Rev. B **50**, 10 722 (1994).
[39]M. S. Hybertsen and S. G. Louie, Phys. Rev. B **34**, 5390 (1986).
[40]M. Rohlfing, P. Krüger, and J. Pollmann, Phys. Rev. B **48**, 17 791 (1993).
[41]M. Alouani, L. Brey, and N. E. Christensen, Phys. Rev. B **37**, 1167 (1988).
[42]P. E. van Camp, V. E. van Doren, and J. T. Devreese, Phys. Rev. B **34**, 1314 (1986).
[43]See, e.g., C. B. Duke, in *Surface Properties of Electronic Materials,* edited by D. A. King and D. P. Woodruff (Elsevier, Amsterdam, 1988), pp. 69–118.
[44]C. B. Duke, S. L. Richardson, A. Paton, and A. Kahn, Surf. Sci. **127**, L135 (1983).
[45]S. Y. Tong, W. N. Wei, and G. Xu, J. Vac. Sci. Technol. B **2**, 393 (1984).
[46]G.-X. Qian, R. M. Martin, and D. J. Chadi, Phys. Rev. B **37**, 1303 (1988).